

# AN ASYMPTOTIC PRESERVING SCHEME FOR KINETIC MODELS WITH SINGULAR LIMIT

ALINA CHERTOCK, CHANGHUI TAN, AND BOKAI YAN

ABSTRACT. We propose a new class of asymptotic preserving schemes to solve kinetic equations with mono-kinetic singular limit. The main idea to deal with the singularity is to transform the equations by appropriate scalings in velocity. In particular, we study two biologically related kinetic systems. We derive the scaling factors, and prove that the rescaled solution does not have a singular limit, under appropriate spatial non-oscillatory assumptions, which can be verified numerically by a newly developed asymptotic preserving scheme. We set up a few numerical experiments to demonstrate the accuracy, stability, efficiency and asymptotic preserving property of the schemes.

## CONTENTS

1. Introduction	2
2. Velocity scaling method	5
2.1. Exact rescaling on spatial “homogeneous” system	5
2.2. Rescaling on the full system with free transport	7
3. Asymptotic behavior	8
3.1. Non-oscillatory assumptions	9
3.2. The scaling factor	10
3.3. The rescaled function	11
4. Asymptotic preserving schemes	14
4.1. AP schemes for the rescaled systems	15
4.2. Asymptotic preserving property	16
5. Numerical experiments	17
5.1. Example 1 – Validation of the assumptions	18
5.2. Example 2 – Consistency test	18
5.3. Example 3 - Asymptotic preserving test	19
5.4. Example 4 – Application	20
References	21

## 1. INTRODUCTION

We consider the following type of kinetic equations,

$$\begin{aligned} \partial_t f_\varepsilon + v \cdot \nabla_x f_\varepsilon &= \frac{1}{\varepsilon} Q(f_\varepsilon), \\ f_\varepsilon(0, x, v) &= f^0(x, v). \end{aligned} \tag{1.1}$$

Here,  $f_\varepsilon = f_\varepsilon(t, x, v)$  is the probability density function at time  $t \geq 0$ , of space variable  $x = (x_1, \dots, x_d)^T \in \Omega$  and velocity  $v = (v_1, \dots, v_d)^T \in \mathbb{R}^d$ , with spatial domain  $\Omega = \mathbb{R}^d$  or  $\mathbb{T}^d$ .  $Q$  is the interaction operator, which can be nonlinear in  $f_\varepsilon$  and nonlocal in  $x$  and  $v$ .

The main property of the interaction operator  $Q$  of our concern is that it has a *mono-kinetic* equilibrium, namely

$$Q(f) = 0 \quad \Leftrightarrow \quad f(t, x, v) = \rho(t, x) \delta_{v=u(t, x)},$$

where  $\delta$  is the Dirac delta distribution, and  $\rho(t, x)$  and  $u(t, x) = (u_1(t, x), \dots, u_d(t, x))^T$  are macroscopic density and velocity, respectively, satisfying

$$\rho(t, x) = \int_{\mathbb{R}^d} f(t, x, v) dv, \quad \rho(t, x) u(t, x) = \int_{\mathbb{R}^d} v f(t, x, v) dv.$$

Under this setup, one can formally let  $\varepsilon \rightarrow 0$  in (1.1) and obtain an asymptotic solution,

$$\lim_{\varepsilon \rightarrow 0} f_\varepsilon(t, x, v) = \rho(t, x) \delta_{v=u(t, x)}, \tag{1.2}$$

which is the equilibrium of  $Q$ , and is singular in  $v$ .

In this paper, we shall focus on the following two interaction operators, both of which have interesting biological applications. The first model is called *aggregation system*, where the interaction operator is defined as

$$\begin{aligned} Q(f)(t, x, v) &= \left[ \int_{\Omega} \int_{\mathbb{R}^d} \nabla_x K(x - y) f(t, y, v^*) dv^* dy \right] \cdot \nabla_v f(t, x, v) \\ &\quad + \nabla_v \cdot (v f(t, x, v)). \end{aligned} \tag{1.3}$$

The operator consists two parts. The first term describes pairwise attraction-repulsion interactions, where  $K$  is the interaction potential. A natural biological assumption is that the strength of the interaction depends on the distance between two agents: attraction in large distance and repulsion in short distance. Hence,  $K = K(r)$  is radial, and it is decreasing when  $r$  is small and increasing when  $r$  is large. The second term represents relaxation in velocity. This term is less biologically motivated, but plays a crucial role in deriving an interesting asymptotic limit [2]. In fact, the mono-kinetic asymptotic solution (1.2) is rigorously derived in [16], see also [10]. Furthermore,  $(\rho, u)$  satisfy

$$\partial_t \rho + \nabla_x \cdot (\rho u) = 0, \quad u(t, x) = - \int_{\Omega} \nabla_x K(x - y) \rho(t, y) dy. \tag{1.4}$$

This limiting system is realized as the *aggregation equation* which appears in various contexts related to biological aggregation models. The equation has been intensively studied in the recent decade, and we refer to [19, 25] and references therein.

The second model is called *3-zone system*, where

$$\begin{aligned} Q(f)(t, x, v) = & \left[ \int_{\Omega} \int_{\mathbb{R}^d} \nabla_x K(x - y) f(t, y, v^*) dv^* dy \right] \cdot \nabla_v f(t, x, v) \\ & + \nabla_v \cdot \left( \int_{\Omega} \int_{\mathbb{R}^d} \phi(|x - y|) (v - v^*) f(y, v^*) f(x, v) dv^* dy \right). \end{aligned} \quad (1.5)$$

The artificial relaxation term in (1.3) is replaced by an *alignment* term, which models pairwise interactions in the middle range. The alignment force, proposed by Cucker and Smale in [7], describes the so called *flocking phenomenon* that agents align their velocities to the neighbors. Here,  $\phi(x)$  is the *influence function* which represents the strength of alignment between two agents. It naturally depends on the distance between the agents, and decreases when the distance becomes larger. We also assume that  $\phi$  is bounded and Lipschitz. Without loss of generality, we take

$$\|\phi\|_{L^\infty} = \phi(0) = 1.$$

The kinetic representation of Cucker-Smale model is derived in [15], analyzed in [4, 24], and numerically studied in [21, 24]. We refer readers to [8, 20] for discussions on Cucker-Smale dynamics with singular influence function.

The interaction operator (1.5) combines long-range attraction, short-range repulsion and mid-range alignment. Such 3-zone interaction framework is proposed in [22]. It has been very successful in biological and ecological modeling, and it is widely used in computer animations. As  $\varepsilon \rightarrow 0$ , the asymptotic limit of (1.1) with interaction (1.5) is rigorously derived in [9], where mono-kinetic asymptotes (1.2) is justified, with  $(\rho, u)$  satisfying

$$\begin{aligned} \partial_t \rho + \nabla_x \cdot (\rho u) &= 0, \\ \int_{\Omega} \phi(|x - y|) \rho(t, y) (u(t, x) - u(t, y)) dy &= - \int_{\Omega} \nabla_x K(x - y) \rho(t, y) dy. \end{aligned} \quad (1.6)$$

The wellposedness theory of the limiting system (1.6) is also established in [9], with the additional equality on momentum conservation. The system serves as a more biologically relevant substitute to the aggregation equation (1.4).

The goal of this paper is to design a universal numerical scheme for (1.1) that solves the equation in both the kinetic regime when  $\varepsilon = \mathcal{O}(1)$ , and the fluid regime when  $\varepsilon \rightarrow 0$ . This type of numerical schemes is called *asymptotic preserving (AP)* and was originally introduced in [17]. The commutative diagram on the left hand side of Figure 1 illustrates the AP property. A scheme  $f_\varepsilon^h$  that approximates the solution  $f_\varepsilon$  with discretization parameters  $h$  is AP if its stability requirement on  $h$  is independent of  $\varepsilon$ , and if its limit  $f^h$  when  $\varepsilon$  tends to zero consistently serves as an approximation of the limiting solution  $f$ . Therefore, the scheme can be automatically applied to the limiting equation simply by setting  $\varepsilon \rightarrow 0$ .

AP schemes have been very successful in solving kinetic equations with different types of hydrodynamic limits, see, e.g., [18] for a recent review of AP schemes. In the conventional kinetic equations and corresponding AP schemes, the limiting profile is usually given by a smooth Maxwellian distribution. Hence one can use fixed grid points in velocity discretization with a cutoff. The study of kinetic equations with non-Maxwellian equilibrium has received attentions recently. AP schemes have been designed for the kinetic equations with heavy-tail equilibrium [5, 6, 26, 27].

The equilibrium of the alignment operator  $Q$  for our system (1.1), on the contrary, is given by a  $\delta$ -distribution in velocity space. As  $\varepsilon$  becomes small, the solution  $f_\varepsilon$  becomes more and more singular. This addresses a major challenge in designing AP schemes for (1.1) as its direct discretization can not achieve high accuracy and stability for small  $\varepsilon$  due to the fact that the limit solution is singular.

To overcome the difficulty, we apply a family of transformations  $\mathcal{T}_\varepsilon$  to the original system (1.1). As illustrated in Figure 1,  $f_\varepsilon$  is mapped to a new function  $g_\varepsilon = \mathcal{T}_\varepsilon[f_\varepsilon]$ . The aim is to find appropriate transformations so that the limiting solution  $g = \lim_{\varepsilon \rightarrow 0} g_\varepsilon$  is not singular, and thus an AP scheme for  $g_\varepsilon$  can be designed without worrying about the singularity.

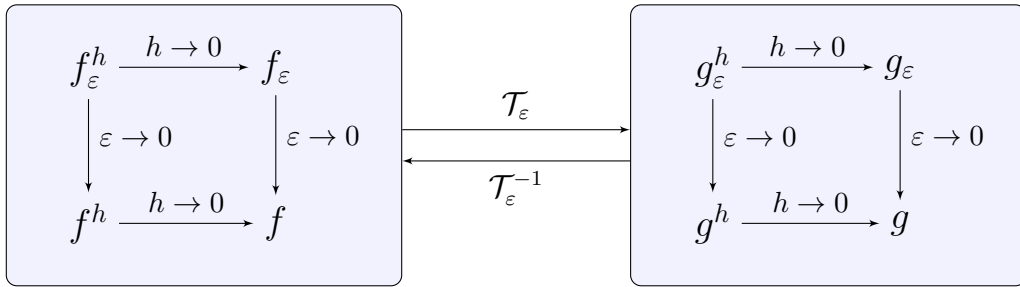


FIGURE 1. AP scheme under transformation

Since the singularity of  $f$  is a  $\delta$ -distribution in velocity, a natural choice of the transformation  $\mathcal{T}_\varepsilon$  is a scaling in velocity. Velocity scaling methods have been used in various kinetic systems with singular time asymptotic limits, see, e.g., [1, 11, 12, 21]. The heart of the matter in these methods is to find an appropriate *scaling factor*  $\omega_\varepsilon$  to ensure that the rescaled function  $g_\varepsilon$  is not singular. In [1, 11, 12], the choice of  $\omega_\varepsilon$  is based on the self-similar behavior of the spatial homogeneous equations, in which the transport part in (1.1) is omitted. The scaling factor used in these works is proven to be optimal only for homogeneous systems with self-similar initial configurations. In [21], a new scaling factor is introduced for kinetic flocking systems and it is shown to be exact for spatially homogeneous systems with all smooth initial conditions.

In this paper, we present an AP scheme for (1.1) based on the velocity scaling method, where the transformation is given by (2.2), with a scaling factor similar to the one proposed in [21]. We study the asymptotic behavior of the rescaled function  $g_\varepsilon$ , and provide sufficient conditions to ensure  $g_\varepsilon$  is non-singular uniformly in  $\varepsilon$ . The result indicates that our choice of scaling factor captures the right scaling. Moreover, it implies that our numerical scheme is indeed asymptotic preserving.

The rest of the paper is organized as follows. In Section 2, we describe the velocity scaling method, and show that with our choice of the scaling factor, the scaling is exact for the spatial “homogeneous” aggregation and 3-zone systems. In Section 3, we discuss the asymptotic behavior of the full system (1.1), and prove that the rescaled profile is not singular under appropriate non-oscillatory conditions. In Section 4, we design AP schemes for the systems after velocity scaling, and discuss the AP property of (1.1). Finally, in Section 5, we provide numerical experiments to illustrate the performance of the new scheme.

## 2. VELOCITY SCALING METHOD

In this section, we present the velocity scaling method for (1.1). We shall follow the storyline of [21] to derive a rescaled system.

**2.1. Exact rescaling on spatial “homogeneous” system.** As the main driving force of the system towards singularity is the interaction operator  $Q$ , we first consider the spatial “homogeneous” system

$$\partial_t f_\varepsilon = \frac{1}{\varepsilon} Q(f_\varepsilon), \quad (2.1)$$

omitting the free transport part. We rescale the velocity variable by

$$\xi = \frac{v - u_\varepsilon}{\omega_\varepsilon},$$

and the transformation  $\mathcal{T}_\varepsilon$  is defined as

$$g_\varepsilon(t, x, \xi) = \mathcal{T}_\varepsilon[f_\varepsilon](t, x, \xi) := \omega_\varepsilon^d f_\varepsilon(t, x, v) = \omega_\varepsilon^d f_\varepsilon(t, x, u_\varepsilon + \omega_\varepsilon \xi). \quad (2.2)$$

Here,  $\omega_\varepsilon = \omega_\varepsilon(t, x)$  is a *scaling factor*, and  $u_\varepsilon = u_\varepsilon(t, x)$  is the macroscopic velocity defined as

$$u_\varepsilon(t, x) = \frac{\int_{\mathbb{R}^d} v f_\varepsilon(t, x, v) dv}{\int_{\mathbb{R}^d} f_\varepsilon(t, x, v) dv}. \quad (2.3)$$

The rescaled function  $g_\varepsilon$  has the following properties. First, the macroscopic density of  $g_\varepsilon$  is the same as the macroscopic density of  $f_\varepsilon$ ,

$$\int_{\mathbb{R}^d} g_\varepsilon(t, x, \xi) d\xi = \int_{\mathbb{R}^d} f_\varepsilon(t, x, v) dv =: \rho_\varepsilon(t, x). \quad (2.4)$$

Second, with the shift by  $u_\varepsilon$ , the first moment of  $g_\varepsilon$  in  $\xi$  is zero for all  $x$ , namely the profile  $g_\varepsilon$  is nicely centered in  $\xi$ ,

$$\int_{\mathbb{R}^d} g_\varepsilon(t, x, \xi) \xi d\xi = 0. \quad (2.5)$$

An appropriate choice of scaling factor  $\omega_\varepsilon$  should produce a *non-singular* rescaled function  $g_\varepsilon$ , which neither concentrates nor spreads out as  $\varepsilon$  approaches zero, namely

$$\max_{\xi} |g_\varepsilon(t, x, \xi)| \leq G, \quad \text{and} \quad \text{supp} g_\varepsilon(t, x, \xi) \subset B_R(0), \quad \forall x \in \Omega, \quad \forall t \in [0, T], \quad (2.6)$$

where  $G$  and  $R$  are finite and independent of  $\varepsilon$ . Here,  $B_R(0)$  denotes for a ball centered at origin and has radius  $R$  in  $(\mathbb{R}^d, |\cdot|_\infty)$ .

To choose an appropriate  $\omega_\varepsilon$ , we represent the dynamics of  $f_\varepsilon$  by the triple  $(g_\varepsilon, u_\varepsilon, \omega_\varepsilon)$ . The term  $\partial_t f_\varepsilon$  can then be expressed by

$$\begin{aligned}\partial_t f_\varepsilon &= -d\omega_\varepsilon^{-d-1}\partial_t\omega_\varepsilon g_\varepsilon + \omega_\varepsilon^{-d}\left[\partial_t g_\varepsilon - \nabla_\xi g_\varepsilon \cdot \frac{\omega_\varepsilon\partial_t u_\varepsilon + (v-u_\varepsilon)\partial_t\omega_\varepsilon}{\omega_\varepsilon^2}\right] \\ &= \omega_\varepsilon^{-d}\left[\partial_t g_\varepsilon - \frac{\partial_t\omega_\varepsilon}{\omega_\varepsilon}\nabla_\xi \cdot (\xi g_\varepsilon) - \omega_\varepsilon^{-1}\partial_t u_\varepsilon \cdot \nabla_\xi g_\varepsilon\right],\end{aligned}\tag{2.7}$$

and the interaction kernel  $Q$  is expressed as

$$Q(f_\varepsilon) = \omega_\varepsilon^{-d}\mathcal{A}_\varepsilon\nabla_\xi \cdot (\xi g_\varepsilon) - \omega_\varepsilon^{-d-1}\mathcal{B}_\varepsilon \cdot \nabla_\xi g_\varepsilon.\tag{2.8}$$

Here,  $\mathcal{A}_\varepsilon = \mathcal{A}_\varepsilon(t, x)$  and  $\mathcal{B}_\varepsilon = \mathcal{B}_\varepsilon(t, x)$  differ for different models. For aggregation system (1.4),

$$\mathcal{A}_\varepsilon(t, x) \equiv 1, \quad \mathcal{B}_\varepsilon(t, x) = -u_\varepsilon(t, x) - \int_\Omega \nabla_x K(x-y)\rho_\varepsilon(t, y)dy.\tag{2.9}$$

For 3-zone system (1.6),

$$\begin{aligned}\mathcal{A}_\varepsilon(t, x) &= \int_\Omega \phi(|x-y|)\rho_\varepsilon(t, y)dy, \\ \mathcal{B}_\varepsilon(t, x) &= \int_\Omega \phi(|x-y|)[u_\varepsilon(t, y) - u_\varepsilon(t, x)]\rho_\varepsilon(t, y)dy \\ &\quad - \int_\Omega \nabla_x K(x-y)\rho_\varepsilon(t, y)dy.\end{aligned}\tag{2.10}$$

Combining (2.7) and (2.8), we obtain an evolution equation for  $g_\varepsilon$

$$\partial_t g_\varepsilon = \left(\frac{\partial_t\omega_\varepsilon}{\omega_\varepsilon} + \frac{1}{\varepsilon}\mathcal{A}_\varepsilon\right)\nabla_\xi \cdot (\xi g_\varepsilon) + \frac{1}{\omega_\varepsilon}\left(\partial_t u_\varepsilon - \frac{1}{\varepsilon}\mathcal{B}_\varepsilon\right) \cdot \nabla_\xi g_\varepsilon.\tag{2.11}$$

To describe the dynamics of  $\rho_\varepsilon$  and  $u_\varepsilon$ , we take zeroth and first moments of  $f_\varepsilon$  in (2.1):

$$\begin{aligned}\frac{\partial}{\partial t}\rho_\varepsilon(t, x) &= \frac{\partial}{\partial t}\int_{\mathbb{R}^d} f_\varepsilon(t, x, v)dv = 0, \\ \frac{\partial}{\partial t}(\rho_\varepsilon(t, x)u(t, x)) &= \frac{\partial}{\partial t}\int_{\mathbb{R}^d} f_\varepsilon(t, x, v)v dv = \frac{1}{\varepsilon}\rho_\varepsilon\mathcal{B}_\varepsilon,\end{aligned}$$

which in turn implies that

$$\rho_\varepsilon(t, x) = \rho^0(x) \quad \text{and} \quad \partial_t u_\varepsilon - \frac{1}{\varepsilon}\mathcal{B}_\varepsilon = 0.\tag{2.12}$$

Therefore, taking into account (2.12) and defining the scaling factor  $\omega_\varepsilon$  in (2.11) as

$$\begin{cases} \partial_t\omega_\varepsilon = -\frac{1}{\varepsilon}\omega_\varepsilon\mathcal{A}_\varepsilon \\ \omega_\varepsilon^0 \equiv 1 \end{cases} \quad \Rightarrow \quad \omega_\varepsilon(t, x) = \exp\left(-\frac{1}{\varepsilon}\int_0^t \mathcal{A}_\varepsilon(s, x)ds\right),\tag{2.13}$$

leads to  $\partial_t g_\varepsilon = 0$ , and thus  $g_\varepsilon$  remains unchanged in all time. In this case, we say that the rescaling is *exact* with factor  $\omega_\varepsilon$ .

Since the initial profile  $f^0(x)$  does not depend on  $\varepsilon$ , it is easy to check that the initial triple  $(g^0, u^0, \omega^0)$  is also independent to  $\varepsilon$ . Hence, the solution  $g(t, x, \xi) = g^0(x, \xi)$  remains the same while  $\varepsilon$  varies and condition (2.6) is clearly satisfied as long as  $g^0$  satisfies (2.6). Moreover, as the scaling is exact, we can easily reconstruct  $f_\varepsilon$  as follows:

$$f_\varepsilon(t, x, v) = e^{dt\mathcal{A}_\varepsilon(t,x)/\varepsilon} f^0\left(x, e^{t\mathcal{A}_\varepsilon(t,x)/\varepsilon}(v - u_\varepsilon(t, x)) + u_\varepsilon^0(x)\right).$$

**Remark 2.1.** In the previous works [11, 12], the scaling factor was chosen to be  $\omega_\varepsilon(t, x) = T_\varepsilon(t, x)^{-1/2}$ , where  $T_\varepsilon$  was the *temperature* of the system, that is,

$$T_\varepsilon(t, x) = \frac{1}{d\rho_\varepsilon(t, x)} \int |v - u_\varepsilon(t, x)|^2 f_\varepsilon(t, x, v) dv.$$

It was also shown that such scaling factor was exact for self-similar initial data. A new scaling factor proposed in [21] takes advantage of the structure of the interaction operator and it is exact for all initial data.

**2.2. Rescaling on the full system with free transport.** We now apply the scaling argument to the full system (1.1). The presence of free transport destroys the self-similar structure of the spatial homogeneous system (2.1) and therefore it is in general impossible to find an exact scaling. We thus extend the idea of the new scaling factor to find a non-singular rescaled function, in the sense of (2.6).

The free transport term can be expressed in terms of  $(g_\varepsilon, u_\varepsilon, \omega_\varepsilon)$  as follows,

$$\begin{aligned} v \cdot \nabla_x f_\varepsilon &= (u_\varepsilon + \omega_\varepsilon \xi) \cdot \left[ -d\omega_\varepsilon^{-d-1} \nabla_x \omega_\varepsilon g_\varepsilon \right. \\ &\quad \left. + \omega_\varepsilon^{-d} \left( \nabla_x g_\varepsilon - \frac{\nabla_x \omega_\varepsilon}{\omega_\varepsilon} (\xi \cdot \nabla_\xi) g_\varepsilon - \frac{1}{\omega_\varepsilon} \sum_{i=1}^d \partial_{\xi_i} g_\varepsilon \nabla_x (u_\varepsilon)_i \right) \right]. \end{aligned}$$

Adding this new contribution to (2.11), yields

$$\begin{aligned} &\partial_t g_\varepsilon + (u_\varepsilon + \omega_\varepsilon \xi) \cdot \nabla_x g_\varepsilon \\ &= \left( \frac{\partial_t \omega_\varepsilon}{\omega_\varepsilon} + (u_\varepsilon + \omega_\varepsilon \xi) \cdot \frac{\nabla_x \omega_\varepsilon}{\omega_\varepsilon} + \frac{1}{\varepsilon} \mathcal{A}_\varepsilon \right) \nabla_\xi \cdot (\xi g_\varepsilon) \\ &\quad + \frac{1}{\omega_\varepsilon} \left( \partial_t u_\varepsilon + (u_\varepsilon + \omega_\varepsilon \xi) \cdot \nabla_x u_\varepsilon - \frac{1}{\varepsilon} \mathcal{B}_\varepsilon \right) \cdot \nabla_\xi g_\varepsilon. \end{aligned} \tag{2.14}$$

Obtaining an exact scaling in this case would require finding a scaling factor  $\omega_\varepsilon$  that satisfies

$$\frac{\partial_t \omega_\varepsilon}{\omega_\varepsilon} + (u_\varepsilon + \omega_\varepsilon \xi) \cdot \frac{\nabla_x \omega_\varepsilon}{\omega_\varepsilon} + \frac{1}{\varepsilon} \mathcal{A}_\varepsilon = 0.$$

Since  $\omega_\varepsilon = \omega_\varepsilon(t, x)$  is independent on the velocity variable  $\xi$ , such  $\omega_\varepsilon$  does not exist. Instead, we take  $\omega_\varepsilon$  which satisfies

$$\partial_t \omega_\varepsilon + u_\varepsilon \cdot \nabla_x \omega_\varepsilon + \frac{1}{\varepsilon} \omega_\varepsilon \mathcal{A}_\varepsilon = 0. \tag{2.15}$$

We again set  $\omega^0(x) \equiv 1$ , namely we do not perform scaling at  $t = 0$ .

By taking the first two moments of (1.1), we deduce the dynamics of macroscopic density  $\rho_\varepsilon$  and velocity  $u_\varepsilon$ :

$$\partial_t \rho_\varepsilon + \nabla_x \cdot (\rho_\varepsilon u_\varepsilon) = 0 \quad (2.16)$$

$$\partial_t (\rho_\varepsilon u_\varepsilon) + \nabla_x \cdot (\rho_\varepsilon u_\varepsilon \otimes u_\varepsilon) + \nabla_x \cdot (\omega_\varepsilon^2 P_\varepsilon) = \frac{1}{\varepsilon} \rho_\varepsilon \mathcal{B}_\varepsilon, \quad (2.17)$$

where  $P_\varepsilon$  is the pressure tensor defined as

$$P_\varepsilon(t, x) := \int_{\mathbb{R}^d} \xi \otimes \xi g_\varepsilon(t, x, \xi) d\xi. \quad (2.18)$$

Note that equation (2.17) can be rewritten in the following non-conservative form:

$$\partial_t u_\varepsilon + u_\varepsilon \cdot \nabla_x u_\varepsilon + \frac{1}{\rho_\varepsilon} \nabla_x \cdot (\omega_\varepsilon^2 P_\varepsilon) = \frac{1}{\varepsilon} \mathcal{B}_\varepsilon, \quad (2.19)$$

and the two forms are equivalent in the non-vacuum region where  $\rho_\varepsilon(x) > 0$ .

Taking into account (2.15), (2.16) and (2.17), equation (2.14) can be rewritten as

$$\begin{aligned} & \partial_t g_\varepsilon + (u_\varepsilon + \omega_\varepsilon \xi) \cdot \nabla_x g_\varepsilon \\ &= (\xi \cdot \nabla_x \omega_\varepsilon) \nabla_\xi \cdot (\xi g_\varepsilon) + ((\xi \cdot \nabla_x) u_\varepsilon) \cdot \nabla_\xi g_\varepsilon - \frac{1}{\rho_\varepsilon \omega_\varepsilon} (\nabla_x \cdot (\omega_\varepsilon^2 P_\varepsilon)) \cdot \nabla_\xi g_\varepsilon, \end{aligned} \quad (2.20)$$

or in the following equivalent conservative form:

$$\partial_t g_\varepsilon + \nabla_x \cdot ((u_\varepsilon + \omega_\varepsilon \xi) g_\varepsilon) = \nabla_\xi \cdot \left[ \left( (\xi \cdot \nabla_x \omega_\varepsilon) \xi + (\xi \cdot \nabla_x) u_\varepsilon - \frac{1}{\rho_\varepsilon \omega_\varepsilon} (\nabla_x \cdot (\omega_\varepsilon^2 P_\varepsilon)) \right) g_\varepsilon \right].$$

Unlike the spatial ‘‘homogeneous’’ system (2.1), the rescaled function  $g_\varepsilon$  does change in time now, and it varies with different  $\varepsilon$ . To validate our choice of scaling factor for the full system, it is important to check that  $g_\varepsilon$  satisfies (2.6) uniformly in  $\varepsilon$ , particularly when  $\varepsilon$  approaches zero.

### 3. ASYMPTOTIC BEHAVIOR

This section is devoted to studying the asymptotic behavior of equations (2.15)–(2.20), as  $\varepsilon \rightarrow 0$ . The goal is to understand whether  $g_\varepsilon$  is non-singular under the proposed rescaling when  $\varepsilon$  is small. The result also supports the AP property of the numerical scheme that will be discussed in Section 4 below.

We denote

$$G_\varepsilon(t) := \max_{x, \xi} |g_\varepsilon(t, x, \xi)|, \quad (3.1)$$

and  $R_\varepsilon(t)$  be the smallest number such that

$$\text{supp}_\xi g_\varepsilon(t, x, \xi) \subset B_{R_\varepsilon(t)}(0). \quad (3.2)$$

We also recall that  $g_\varepsilon$  is non-singular if condition (2.6) is satisfied and hence we shall show that  $G_\varepsilon(t)$  and  $R_\varepsilon(t)$  are bounded independent of  $\varepsilon$ , for all  $t \in [0, T]$ , under appropriate assumptions.



**3.1. Non-oscillatory assumptions.** We start our discussion with two assumptions on the solution triple  $(g_\varepsilon, u_\varepsilon, \omega_\varepsilon)$ . The first one is a spatially non-oscillatory assumption on the rescaled function  $g_\varepsilon$ ,

$$|\nabla_x g_\varepsilon(t, x, \xi)| \leq C_1 g_\varepsilon(t, x, \xi), \quad (3.3)$$

for all  $t \in [0, T]$ ,  $x \in \Omega$  and  $\xi \in \mathbb{R}^d$ , where the constant  $C_1$  is uniform in  $\varepsilon$ . Condition (3.3) implies non-oscillatory bounds on macroscopic quantities. Indeed, for density  $\rho_\varepsilon$ , we have

$$|\nabla_x \rho_\varepsilon(t, x)| = \left| \int \nabla_x g_\varepsilon(t, x, \xi) d\xi \right| \leq C_1 \rho_\varepsilon(t, x). \quad (3.4)$$

For pressure  $P_\varepsilon$ , we have the following estimate

$$|P_\varepsilon(t, x)| = \left| \int \xi \otimes \xi g_\varepsilon(t, x, \xi) d\xi \right| \leq R_\varepsilon^2(t) \rho_\varepsilon(t, x), \quad (3.5)$$

and condition (3.3) implies

$$|\nabla_x P_\varepsilon(t, x)| = \left| \int \xi \otimes \xi \nabla_x g_\varepsilon(t, x, \xi) d\xi \right| \leq C_1 R_\varepsilon^2(t) \rho_\varepsilon(t, x). \quad (3.6)$$

If condition (3.3) is violated, then  $g_\varepsilon$  becomes more oscillatory when  $\varepsilon$  gets smaller, in which case one can not expect to design AP numerical scheme for  $g_\varepsilon$ .

The second assumption is the Lipschitz a priori bound on the macroscopic velocity  $u_\varepsilon$ ,

$$\|\nabla_x u_\varepsilon(t, \cdot)\|_{L^\infty(\Omega)} \leq C_2 < \infty, \quad (3.7)$$

for all  $t \in [0, T]$ , where the constant  $C_2$  is uniform in  $\varepsilon$ .

It should be observed that taking  $\varepsilon \rightarrow 0$  in (2.16) and (2.19), one can formally obtain the limiting system, for which condition (3.7) is also satisfied. The argument has been rigorously proved in [16] for the aggregation system (1.4) and in [9] for the 3-zone system (1.6). For both systems, the limiting velocity  $u$  is Lipschitz globally in time, under suitable regularity assumptions on kernels  $K$  and  $\phi$ , and thus satisfies (3.7). The regularity for the limiting system does not imply, however, that (3.7) holds uniformly in  $\varepsilon$ . In fact, the convergence of  $f_\varepsilon$  to  $\rho \delta_{v=u}$  is only weak-\* in measure. This does not rule out the possibility of oscillation in  $x$  as  $\varepsilon \rightarrow 0$ .

In [3, 23], it has also been proven that condition (3.7) is satisfied when the system (2.16), (2.19) is considered in the pressureless regime and does not depend on  $g_\varepsilon$ , i.e.,

$$\partial_t \rho_\varepsilon + \nabla_x \cdot (\rho_\varepsilon u_\varepsilon) = 0, \quad \partial_t u_\varepsilon + u_\varepsilon \cdot \nabla_x u_\varepsilon = \frac{1}{\varepsilon} \mathcal{B}_\varepsilon, \quad (3.8)$$

and subject to subcritical initial data. Moreover, the subcritical region becomes larger when  $\varepsilon$  gets smaller. Therefore, (3.7) is satisfied uniformly for  $\varepsilon \in [0, \varepsilon_0]$  if the initial profile  $u^0$  lies in the subcritical region of the system (3.8) with  $\varepsilon = \varepsilon_0$ .

The result for pressureless system (3.8) can be easily extended to the general dynamics (2.19) when the pressure term is Lipschitz bounded uniformly in  $\varepsilon$ . Indeed, from (3.5) and (3.6), we know  $P_\varepsilon/\rho_\varepsilon$  and  $\nabla_x P_\varepsilon/\rho_\varepsilon$  are uniformly bounded by  $R_\varepsilon^2$ . This together with the estimate on  $\omega_\varepsilon$  (see Section 3.2) implies boundedness of the

pressure term in (2.19). The Lipschitz bound can also be obtained by the additional non-oscillatory assumption

$$|\nabla_x^{\otimes 2} g_\varepsilon(t, x, \xi)| \lesssim g_\varepsilon(t, x, \xi).$$

We omit the proof and redirect the reader to [3, 23] for relevant discussions.

We have thus argued that condition (3.7) holds under appropriate setup if  $g_\varepsilon$  is non-oscillatory in  $x$ . Therefore, both (3.3) and (3.7) are considered as spatially non-oscillatory assumptions on  $g_\varepsilon$ . Given these two assumptions, we are going to prove that  $g_\varepsilon$  is non-singular, uniformly in  $\varepsilon$ .

**3.2. The scaling factor.** In this section, we use the evolution equation (2.15) to estimate both the scaling factor  $\omega_\varepsilon$  and its gradient  $\nabla_x \omega_\varepsilon$ . To this end, we begin with the following proposition.

**Proposition 3.1.** *Assume  $\mathcal{A}_\varepsilon$  is bounded below by a positive constant  $c$  that is independent of  $\varepsilon$ , then  $\|\omega_\varepsilon(t, \cdot)\|_{L^\infty(\Omega)}$  tends to 0 as  $\varepsilon \rightarrow 0$ .*

*Proof.* Consider a flow map  $X_\varepsilon(t, x)$  such that

$$\partial_t X_\varepsilon(t, x) = u_\varepsilon(t, X_\varepsilon(t, x)), \quad X_\varepsilon(0, x) = x. \quad (3.9)$$

Along each characteristic path, we have

$$\frac{d}{dt} \omega_\varepsilon(t, X_\varepsilon(t, x)) = -\frac{1}{\varepsilon} (\omega_\varepsilon \mathcal{A}_\varepsilon)(t, X_\varepsilon(t, x)),$$

which in turns yields

$$\omega_\varepsilon(t, X_\varepsilon(t, x)) = \omega^0(x) \exp\left(-\frac{1}{\varepsilon} \int_0^t \mathcal{A}_\varepsilon(s, X_\varepsilon(s, x)) ds\right) \leq \exp\left(-\frac{c}{\varepsilon} t\right).$$

Collecting all paths, we obtain

$$\|\omega_\varepsilon(t, \cdot)\|_{L^\infty(\Omega)} \leq \exp\left(-\frac{c}{\varepsilon} t\right), \quad (3.10)$$

which vanishes as  $\varepsilon \rightarrow 0$ .  $\square$

**Remark 3.1.** Since  $\lim_{\varepsilon \rightarrow 0} f_\varepsilon$  is singular, a correct rescaling has to have a factor  $\omega_\varepsilon$  vanishes as  $\varepsilon \rightarrow 0$ . This is true for our choice of  $\omega_\varepsilon$ .

**Remark 3.2.** Under appropriate settings, the lower bound assumption on  $\mathcal{A}_\varepsilon$  is valid for both the aggregation system (2.9) and 3-zone system (2.10). Indeed, for the aggregation system,  $\mathcal{A}_\varepsilon \equiv 1$ , while for the 3-zone system,  $\mathcal{A}_\varepsilon$  can be estimated by

$$\mathcal{A}_\varepsilon(t, x) = \int_\Omega \phi(|x - y|) \rho_\varepsilon(t, y) dy \geq \phi_{\min} \|\rho_\varepsilon(t, \cdot)\|_{L^1(\Omega)} = \phi_{\min},$$

provided  $\phi$  is lower bounded by  $\phi_{\min} > 0$ . Note that  $\|\rho_\varepsilon(t, \cdot)\|_{L^1(\Omega)} = 1$  due to mass conservation, and the fact that  $f_\varepsilon$  is a probability distribution. The assumption on  $\phi$  can be further relaxed (see e.g. [23]). We omit the details.

Next, we provide a bound on  $\nabla_x \omega_\varepsilon$ , which is only needed for the 3-zone system (2.10), as the quantity is identically zero in aggregation system (2.9).

**Proposition 3.2.** *For the 3-zone system (2.10), we have  $\|\nabla_x \mathcal{A}_\varepsilon\|_{L^\infty(0,T;\Omega)} \leq C_1$ . Moreover,  $\|\nabla_x \omega_\varepsilon\|_{L^\infty(0,T;\Omega)}$  tends to 0 as  $\varepsilon \rightarrow 0$ .*

*Proof.* We start with the estimate on  $\nabla_x \mathcal{A}_\varepsilon$  and obtain from (2.10):

$$\begin{aligned} |\nabla_x \mathcal{A}_\varepsilon(t, x)| &= \left| \int \phi(|x - y|) \nabla_x \rho_\varepsilon(t, y) dy \right| \\ &\leq C_1 \int \phi(|x - y|) \rho_\varepsilon(t, y) dy \leq C_1 \|\phi\|_{L^\infty} \|\rho_\varepsilon(t, \cdot)\|_{L^1} = C_1, \end{aligned}$$

where the first inequality is due to non-oscillatory condition (3.4). Here, we recall our assumption that  $\phi$  is bounded and  $\|\phi\|_{L^\infty} = 1$ .

We now estimate  $\nabla_x \omega_\varepsilon$  by applying operator  $\nabla_x$  to equation (2.15). Once again we consider the flow map (3.9) and obtain the following equation along each characteristic path:

$$\frac{d}{dt} \nabla_x \omega_\varepsilon(t, X_\varepsilon(t, x)) = -\frac{1}{\varepsilon} \nabla_x (\omega_\varepsilon \mathcal{A}_\varepsilon) - \sum_{j=1}^d \partial_{x_j} \omega_\varepsilon \nabla_x (u_\varepsilon)_j.$$

Denote  $M_\varepsilon(t, x) := |\nabla_x \omega_\varepsilon(t, x)|_\infty$ , where  $|\cdot|_\infty$  is the infinity norm in  $\mathbb{R}^d$ . Then,

$$\frac{d}{dt} M_\varepsilon(t, X_\varepsilon(t, x)) \leq \left( -\frac{c}{\varepsilon} + |\nabla_x u_\varepsilon(t, X_\varepsilon(t, x))|_\infty \right) M_\varepsilon + \frac{C_1}{\varepsilon} \omega_\varepsilon(t, X_\varepsilon(t, x)).$$

This implies

$$\begin{aligned} M_\varepsilon(t, X_\varepsilon(t, x)) &\leq M(0, x) \exp \left[ \int_0^t \left( -\frac{c}{\varepsilon} + |\nabla_x u_\varepsilon(s, X_\varepsilon(s, x))|_\infty \right) ds \right] \\ &\quad + \frac{C_1}{\varepsilon} \int_0^t \omega_\varepsilon(s, X_\varepsilon(s, x)) \exp \left[ \int_s^t \left( -\frac{c}{\varepsilon} + |\nabla_x u_\varepsilon(\tau, X_\varepsilon(\tau, x))|_\infty \right) d\tau \right] ds. \end{aligned}$$

As  $\omega^0(x) \equiv 1$ , we obtain  $M(0, x) \equiv 0$ .

Given any  $t \in [0, T]$ , we combine all paths and use (3.7) (3.10), to obtain

$$\begin{aligned} \|M_\varepsilon(t, \cdot)\|_{L^\infty} &\leq \frac{C_1}{\varepsilon} \int_0^t \exp \left( -\frac{c}{\varepsilon} s \right) \exp \left[ -\frac{c(t-s)}{\varepsilon} + C_2(t-s) \right] ds \\ &= \frac{C_1(e^{C_2 t} - 1)}{C_2 \varepsilon} \exp \left( -\frac{c}{\varepsilon} t \right), \end{aligned}$$

which also vanishes as  $\varepsilon \rightarrow 0$ . □

**3.3. The rescaled function.** We now investigate regularity properties of function  $g_\varepsilon$  in the sense of (2.6).

**Proposition 3.3.** *Consider functions  $G_\varepsilon(t)$  and  $R_\varepsilon(t)$  defined in (3.1) and (3.2), respectively. Suppose  $R_\varepsilon(t)$  is uniformly bounded in  $\varepsilon$ , for  $t \in [0, T]$ . Then,  $G_\varepsilon(t)$  is also uniformly bounded in  $\varepsilon$  for  $t \in [0, T]$ .*

*Proof.* Consider a flow map  $(X_\varepsilon(t, x, \xi), \Xi_\varepsilon(t, x, \xi))$  in  $(x, \xi)$  plane, where

$$\begin{aligned} \partial_t X_\varepsilon(t, x, \xi) &= u_\varepsilon(t, X_\varepsilon) + \omega_\varepsilon(t, X_\varepsilon)\Xi_\varepsilon, \\ \partial_t \Xi_\varepsilon(t, x, \xi) &= (\Xi_\varepsilon \cdot \nabla_x \omega_\varepsilon(t, X_\varepsilon))\Xi_\varepsilon + (\Xi_\varepsilon \cdot \nabla_x)u_\varepsilon(t, X_\varepsilon) \\ &\quad - \frac{1}{\rho_\varepsilon(t, X_\varepsilon)\omega_\varepsilon(t, X_\varepsilon)} \nabla_x \cdot (\omega_\varepsilon^2(t, X_\varepsilon)P_\varepsilon(t, x)), \\ X_\varepsilon(0, x, \xi) &= x, \quad \Xi_\varepsilon(0, x, \xi) = \xi. \end{aligned} \tag{3.11}$$

From (2.20), along each characteristic path we have

$$\frac{d}{dt}g_\varepsilon(t, X_\varepsilon(t, x, \xi), \Xi_\varepsilon(t, x, \xi)) = d(\Xi_\varepsilon \cdot \nabla_x \omega_\varepsilon(t, X_\varepsilon))g_\varepsilon(t, X_\varepsilon, \Xi_\varepsilon).$$

Therefore, if  $(x, \xi) \notin \text{supp}(g^0)$ , then  $g_\varepsilon(t, X_\varepsilon, \Xi_\varepsilon) = 0$ . If  $(x, \xi) \in \text{supp}(g^0)$ , then

$$\begin{aligned} g_\varepsilon(t, X_\varepsilon, \Xi_\varepsilon) &= g^0(x, \xi) \exp \left[ d \int_0^t \Xi_\varepsilon(s, x, \xi) \cdot \nabla_x \omega_\varepsilon(t, X_\varepsilon(s, x)) ds \right] \\ &\leq G(0) \exp \left[ d \int_0^t R_\varepsilon(s) \|\nabla_x \omega_\varepsilon(s, \cdot)\|_{L^\infty(\Omega)} ds \right]. \end{aligned}$$

Taking the supreme on all  $(X_\varepsilon, \Xi_\varepsilon)$ , yields

$$G_\varepsilon(t) \leq G(0) \exp \left[ d \int_0^t R_\varepsilon(s) \|\nabla_x \omega_\varepsilon(s, \cdot)\|_{L^\infty(\Omega)} ds \right].$$

Note that  $G(0)$  does not depend on  $\varepsilon$  and therefore, from Proposition 3.2 and the assumption that  $R_\varepsilon(t)$  is bounded uniformly in  $\varepsilon$ , it follows that  $G_\varepsilon(t)$  is also uniformly bounded in  $\varepsilon$ .  $\square$

**Remark 3.3.** It follows from Proposition 3.3 that if the rescaled function  $g_\varepsilon$  does not spread out, it will not concentrate either. In particular, for the aggregation system (2.9) there is no concentration regardless of the size of the support of  $g_\varepsilon$  since  $\nabla_x \omega_\varepsilon \equiv 0$  in this case.

We are left to prove that  $g_\varepsilon$  does not spread out. The growth of the support of  $g_\varepsilon$  is equivalent to the spread of the characteristic paths in (3.11), whose dynamics implies the following estimate on  $R_\varepsilon(t)$ :

$$\begin{aligned} \frac{d}{dt}R_\varepsilon(t) &\leq \|\nabla_x \omega_\varepsilon(t, \cdot)\|_{L^\infty(\Omega)} R_\varepsilon(t)^2 + \|\nabla_x u_\varepsilon(t, \cdot)\|_{L^\infty(\Omega)} R_\varepsilon(t) \\ &\quad + 2\|\nabla_x \omega_\varepsilon(t, \cdot)\|_{L^\infty(\Omega)} \max_{x \in \Omega} \frac{|P_\varepsilon(t, x)|_\infty}{\rho_\varepsilon(t, x)} + \|\omega_\varepsilon(t, \cdot)\|_{L^\infty(\Omega)} \max_{x \in \Omega} \frac{|\nabla_x P_\varepsilon(t, x)|_\infty}{\rho_\varepsilon(t, x)}. \end{aligned}$$

From the non-oscillatory bounds (3.5)–(3.7), we obtain

$$\frac{d}{dt}R_\varepsilon(t) \leq (3\|\nabla_x \omega_\varepsilon(t, \cdot)\|_{L^\infty(\Omega)} + C_1\|\omega_\varepsilon(t, \cdot)\|_{L^\infty(\Omega)})R_\varepsilon(t)^2 + C_2R_\varepsilon(t).$$

The estimate has the form

$$\frac{d}{dt}R_\varepsilon(t) \leq a_\varepsilon(t)R_\varepsilon(t)^2 + C_2R_\varepsilon(t), \quad (3.12)$$

where  $a_\varepsilon$  can be determined by Propositions 3.1 and 3.2.

The last inequality (3.12) allows us to prove that under appropriate assumptions on  $\varepsilon$  and  $R(0)$ , the function  $R_\varepsilon(t)$  in (3.2) is bounded globally in time.

**Proposition 3.4.** *There exist  $\varepsilon_0 > 0$  and  $R^0 > 0$  such that for all  $\varepsilon \in (0, \varepsilon_0]$ , function  $R_\varepsilon(t)$  defined in (3.2) is bounded for any finite time  $t$  for both the aggregation system (2.9) and 3-zone system (2.10) provided  $R(0) \leq R^0$ .*

*Proof.* We first consider aggregation system (2.9). From the estimate (3.10) and the fact that  $\nabla_x \omega_\varepsilon = 0$ , we have

$$a_\varepsilon(t) = C_1 \exp\left(-\frac{c}{\varepsilon}t\right).$$

We denote  $S_\varepsilon(t) := R_\varepsilon(t) \exp(-\frac{c}{\varepsilon}t)$  and obtain from (3.12) the dynamics of  $S_\varepsilon$ :

$$\frac{d}{dt}S_\varepsilon(t) \leq C_1S_\varepsilon(t)^2 - \left(\frac{c}{\varepsilon} - C_2\right)S_\varepsilon(t).$$

We now take  $\varepsilon_0 = \frac{c}{2C_2}$  and  $R^0 = \frac{C_2}{C_1}$  and observe that since  $c - C_2\varepsilon > 0$ ,  $S_\varepsilon$  has an invariant region  $\left[0, \frac{c - C_2\varepsilon}{C_1\varepsilon}\right]$  and the following inequality holds:

$$S(0) = R(0) \leq R^0 = \frac{C_2}{C_1} = \frac{c - C_2\varepsilon_0}{C_1\varepsilon_0} \leq \frac{c - C_2\varepsilon}{C_1\varepsilon}.$$

Therefore,  $S_\varepsilon(t) \leq \frac{c - C_2\varepsilon}{C_1\varepsilon}$  for all  $t \geq 0$  and we conclude with the bound

$$R_\varepsilon(t) = S_\varepsilon(t) \exp\left(\frac{c}{\varepsilon}t\right) \leq \frac{c - C_2\varepsilon}{C_1\varepsilon} \exp\left(\frac{c}{\varepsilon}t\right).$$

Next, we turn our attention to the 3-zone system (2.10). By propositions 3.1 and 3.2, we have

$$a_\varepsilon(t) = C_1 \exp\left(-\frac{c}{\varepsilon}t\right) \left(1 + \frac{3(e^{C_2t} - 1)}{C_2\varepsilon}\right). \quad (3.13)$$

The extra exponential growth  $e^{C_2t}$  in (3.13) is due to the estimate of  $\nabla_x \omega_\varepsilon$ . It can be controlled by the exponential decay provided  $C_2 < \frac{c}{\varepsilon}$ . In fact, we have

$$a_\varepsilon(t) \leq \tilde{C}_1 \exp\left(-\frac{c - C_2\varepsilon}{\varepsilon}t\right), \quad \text{where } \tilde{C}_1 = \max\left\{\frac{3C_1}{C_2\varepsilon}, C_1\right\}.$$

Using the same argument as the aggregation system, we obtain the following bound:

$$R_\varepsilon(t) \leq \frac{c - 2C_2\varepsilon}{\tilde{C}_1\varepsilon} \exp\left(\frac{c - C_2\varepsilon}{\varepsilon}t\right)$$

as long as  $\varepsilon < \varepsilon_0 = \frac{c}{4C_2}$  and  $R(0) \leq R^0 = \frac{C_2}{6C_1} \cdot \min\{c, 12\}$ .  $\square$

It should be pointed out that the two bounds obtained above are not uniform in  $\varepsilon$ . Uniform bounds can only be achieved up to a finite time, provided that  $a_\varepsilon(t)$  is uniformly bounded.

**Proposition 3.5.** *There exists a time  $T > 0$ , such that  $R_\varepsilon(t)$  is bounded in  $t \in [0, T]$ , uniformly in  $\varepsilon$ .*

*Proof.* For the aggregation system (2.9),  $a_\varepsilon(t)$  is uniformly bounded by  $C_1$  and from (3.12) we have

$$\frac{d}{dt}R_\varepsilon(t) \leq C_1R_\varepsilon(t)^2 + C_2R_\varepsilon(t),$$

which is a Ricatti-type first order ODE. Therefore, there exists a finite time  $T = T(C_1, C_2, R(0)) > 0$ , such that  $R_\varepsilon(t)$  remains finite in  $[0, T]$ . Since  $T$  does not depend on  $\varepsilon$ , the bound is uniformly in  $\varepsilon$ .

For the 3-zone system (2.10), we use the estimate (3.13) to obtain

$$a_\varepsilon(t) \leq C_1 + \frac{3C_1(e^{C_2t} - 1)}{C_2} \cdot \frac{1}{\varepsilon} \exp\left(-\frac{c}{\varepsilon}t\right).$$

The  $\frac{1}{\varepsilon}$  term can be controlled by the exponentially decay, namely,

$$\frac{1}{\varepsilon} \exp\left(-\frac{c}{\varepsilon}t\right) \leq \frac{1}{cet},$$

for all  $\varepsilon \in [0, \infty)$ , which in turns implies

$$a_\varepsilon(t) \leq C_1 + \frac{3C_1}{C_2ce} \cdot \frac{e^{C_2t} - 1}{t}.$$

The right hand side in the last inequality is an increasing function in  $t$ . Therefore, we conclude that  $a_\varepsilon(t)$  is bounded by  $C_1 + \frac{3C_1}{C_2ce} \cdot \frac{e^{C_2T} - 1}{T}$ , which does not depend on  $\varepsilon$ , and thus according to (3.12),  $R_\varepsilon(t)$  is uniformly bounded in  $\varepsilon$  for any finite time  $t \in [0, T]$ .  $\square$

Putting everything together, we prove that  $g_\varepsilon$  is non-singular. It provides a strong support that our choice of  $\omega_\varepsilon$  captures the right scaling.

**Theorem 3.6.** *Let  $(g_\varepsilon, u_\varepsilon, \omega_\varepsilon)$  be the solution triple of the rescaled dynamics (2.15), (2.17) and (2.20). Assume the solution satisfies the non-oscillatory conditions (3.3) and (3.7). Then, there exists a time  $T = T(g^0) > 0$ , such that  $g_\varepsilon(t)$  is non-singular uniformly in  $\varepsilon$  in the sense of (2.6), for all  $t \in [0, T]$ .*

#### 4. ASYMPTOTIC PRESERVING SCHEMES

Now we design a asymptotic preserving scheme to solve (1.1). To avoid the singularity limit, we use velocity scaling method and express the solution  $f_\varepsilon$  by the rescaled function  $g_\varepsilon$ , together with the scaling factor  $\omega_\varepsilon$  and macroscopic velocity  $u_\varepsilon$ . We have shown in Theorem 3.6 that under our proposed rescaling,  $g_\varepsilon$  is non-singular

uniformly in  $\varepsilon$ . Therefore, we proceed to design AP schemes for the rescaled system, where singularity is no longer an obstacle.

**4.1. AP schemes for the rescaled systems.** Let us recall the dynamics of the solution triple  $(g_\varepsilon, u_\varepsilon, \omega_\varepsilon)$  and rewrite equations (2.15), (2.17) and (2.20) in the numerical friendly conservative representations,

$$\begin{cases} \partial_t g_\varepsilon + \nabla_x \cdot ((u_\varepsilon + \omega_\varepsilon \xi) g_\varepsilon) \\ \quad = \nabla_\xi \cdot \left[ \left( (\xi \cdot \nabla_x \omega_\varepsilon) \xi + (\xi \cdot \nabla_x) u_\varepsilon - \frac{1}{\rho_\varepsilon \omega_\varepsilon} (\nabla_x \cdot (\omega_\varepsilon^2 P_\varepsilon)) \right) g_\varepsilon \right], \\ \partial_t (\rho_\varepsilon u_\varepsilon) + \nabla_x \cdot (\rho_\varepsilon u_\varepsilon \otimes u_\varepsilon) + \nabla_x \cdot (\omega_\varepsilon^2 P_\varepsilon) = \frac{1}{\varepsilon} \rho_\varepsilon \mathcal{B}_\varepsilon, \\ \partial_t \omega_\varepsilon + u_\varepsilon \cdot \nabla_x \omega_\varepsilon + \frac{1}{\varepsilon} \omega_\varepsilon \mathcal{A}_\varepsilon = 0. \end{cases} \quad (4.1)$$

with  $\rho_\varepsilon(t, x)$  defined in (2.4) and satisfying the continuity equation (2.16).

To obtain an AP scheme for system (4.1), we introduce an increasing sequence  $0 < t^0 < t^1 \dots < t^n \dots$  of times with uniform time step  $\Delta t = t^{n+1} - t^n$  and denote by  $q^n$  the value of any unknown quantity  $q$  at time  $t^n$ , i.e.,  $q^n(\cdot) \approx q(t^n, \cdot)$ . The canonical first order in time explicit-implicit time discretization for (4.1) reads:

$$\begin{cases} \frac{g_\varepsilon^{n+1} - g_\varepsilon^n}{\Delta t} + \nabla_x \cdot ((u_\varepsilon^n + \omega_\varepsilon^n \xi) g_\varepsilon^n) \\ \quad = \nabla_\xi \cdot \left[ \left( (\xi \cdot \nabla_x \omega_\varepsilon^n) \xi + (\xi \cdot \nabla_x) u_\varepsilon^n - \frac{1}{\rho_\varepsilon^n \omega_\varepsilon^n} (\nabla_x \cdot ((\omega_\varepsilon^n)^2 P_\varepsilon^n)) \right) g_\varepsilon^n \right], \\ \frac{\rho_\varepsilon^{n+1} u_\varepsilon^{n+1} - \rho_\varepsilon^n u_\varepsilon^n}{\Delta t} + \nabla_x \cdot (\rho_\varepsilon^n u_\varepsilon^n \otimes u_\varepsilon^n) + \nabla_x \cdot ((\omega_\varepsilon^n)^2 P_\varepsilon^n) = \frac{\rho_\varepsilon^{n+1}}{\varepsilon} \mathcal{B}_\varepsilon^{n+1}, \\ \frac{\omega_\varepsilon^{n+1} - \omega_\varepsilon^n}{\Delta t} + u_\varepsilon^n \cdot \nabla_x \omega_\varepsilon^n + \frac{1}{\varepsilon} \omega_\varepsilon^{n+1} \mathcal{A}_\varepsilon^{n+1} = 0, \end{cases} \quad (4.2)$$

where the non-stiff fluxes are treated explicitly and the stiff terms are treated implicitly. To evolve the solution in time, we first compute  $g_\varepsilon^{n+1}$  from the first equation in (4.2), which is fully explicit as  $g_\varepsilon$  is non-singular, and its dynamics does not explicitly depend on  $\varepsilon$ . Then,  $\rho_\varepsilon^{n+1}$  is obtained from the integration of  $g_\varepsilon^{n+1}$  in  $\xi$  coordinate. Next, we use an implicit solver to compute  $\rho_\varepsilon^{n+1} u_\varepsilon^{n+1}$  from the second equation. Noting that the operator  $\rho_\varepsilon \mathcal{B}_\varepsilon$  is a symmetric operator on  $\rho_\varepsilon u_\varepsilon$ , one can simply apply a conjugate-gradient method. Finally,  $\omega_\varepsilon^{n+1}$  can be obtained easily from the third equation since  $\mathcal{A}_\varepsilon^{n+1}$  only depends on  $\rho_\varepsilon^{n+1}$  and hence can be computed explicitly.

One can derive a second order time discretization scheme by applying, say, a backward differentiation formula (BDF) on the time derivative, an extrapolation on the explicit terms and a fully implicit solver on the stiff terms. We omit the details here and refer the reader to [13, 14, 26].

A fully discrete scheme should be obtained by consistent spatial and velocity discretizations, for instance, by using a finite volume method thanks to the conservative structure of the equations; see, e.g., [21] for the references. Importantly, since  $g_\varepsilon$  is non-singular, the discretizations are independent of  $\varepsilon$ .

We summarize the entire procedure of the proposed numerical approach for solving (1.1). Given initial data  $f^0$ , we set  $\omega^0 \equiv 1$ , compute  $u^0$  by (2.3) and  $g^0$  by performing velocity scaling transformation  $\mathcal{T}_\varepsilon$  in (2.2). Then, we evolve the dynamics (4.1) on  $(g_\varepsilon, u_\varepsilon, \omega_\varepsilon)$  using appropriate AP scheme, for instance (4.2), until a target time  $t$ . Finally, we apply the inverse transformation  $\mathcal{T}_\varepsilon^{-1}$  to obtain the solution  $f_\varepsilon$  at time  $t$ . Note that  $\mathcal{T}_\varepsilon^{-1}$  has an explicit form

$$f_\varepsilon(t, x, v) = \mathcal{T}_\varepsilon^{-1}[g_\varepsilon](t, x, v) = \frac{1}{\omega_\varepsilon(t, x)^d} g_\varepsilon \left( t, x, \frac{v - u_\varepsilon(t, x)}{\omega_\varepsilon(t, x)} \right), \quad (4.3)$$

which is easy to implement numerically.

**4.2. Asymptotic preserving property.** Now, we verify the AP property of our numerical scheme.

Recall the limiting system of (1.1) as  $\varepsilon \rightarrow 0$  satisfies mono-kinetic asymptotes (1.2)  $f(t, x, v) = \rho(t, x)\delta_{v=u(t, x)}$ , with macroscopic quantities  $(\rho, u)$  satisfying

$$\partial_t \rho + \nabla_x \cdot (\rho u) = 0, \quad \rho \mathcal{B} = 0. \quad (4.4)$$

The goal is to check that  $f_\varepsilon^n$  converges to  $f^n$  as  $\varepsilon \rightarrow 0$ , at the discrete level.

As discussed in Section 3, the spatial non-oscillatory conditions (3.3) and (3.7) play an important role and guarantee that  $g_\varepsilon$  is non-singular, in the sense of (2.6). This argument, stated in Theorem 3.6, can be extended to semi-discrete or fully discrete dynamics with appropriate choices of discretizations.

We shall consider the first order scheme (4.2) as an example. The semi-discrete version of Theorem 3.6 implies that  $g_\varepsilon^n$  is non-singular, namely

$$\max_\xi |g_\varepsilon^n(x, \xi)| \leq G, \quad \text{and} \quad \text{supp}_\xi g_\varepsilon^n(x, \xi) \subset B_R(0), \quad \forall x \in \Omega, \quad (4.5)$$

where  $G, R$  are constants independent of  $\varepsilon$ , if

$$|\nabla_x g_\varepsilon^n(x, \xi)| \leq C_1 g_\varepsilon^n(x, \xi), \quad \|\nabla_x u_\varepsilon^n\|_{L^\infty(\Omega)} \leq C_2, \quad (4.6)$$

for all  $x \in \Omega, \xi \in \mathbb{R}^d$ , where  $C_1, C_2$  are constants which do not depend on  $\varepsilon$ .

Assuming (4.6) holds, we, first, check  $f_\varepsilon^n$  converges to a mono-kinetic profile as  $\varepsilon \rightarrow 0$ . It is enough to show that for any given  $x \in \Omega$ , the size of  $\text{supp}_v f_\varepsilon^n(x, v)$  tends to 0 as  $\varepsilon \rightarrow 0$ . From (4.3) and (4.5), we obtain

$$|\text{supp}_v f_\varepsilon^n(x, v)| = \omega_\varepsilon^n(x) |\text{supp}_\xi g_\varepsilon^n(x, \xi)| \leq 2R\omega_\varepsilon^n(x).$$

A semi-discrete version of proposition 3.1 implies that  $\omega_\varepsilon^n(x) \rightarrow 0$  as  $\varepsilon \rightarrow 0$ , which finishes the proof. Indeed,

$$\|\omega_\varepsilon^n\|_{L^\infty(\Omega)} \leq \frac{\|\omega_\varepsilon^{n-1}\|_{L^\infty(\Omega)}}{1 + \frac{\Delta t}{\varepsilon} \mathcal{A}^n} \leq \frac{\|\omega_\varepsilon^{n-1}\|_{L^\infty(\Omega)}}{1 + \frac{c\Delta t}{\varepsilon}} \leq \dots \leq \frac{\|\omega^0\|_{L^\infty(\Omega)}}{\left(1 + \frac{c\Delta t}{\varepsilon}\right)^n} \leq \exp\left(-\frac{ct}{\varepsilon}\right) \xrightarrow{\varepsilon \rightarrow 0} 0.$$

Here,  $\mathcal{A}_\varepsilon^n \geq c$  due to Remark 3.2.



Next, we show that the macroscopic quantities  $(\rho_\varepsilon^n, u_\varepsilon^n)$  converges to  $(\rho^n, u^n)$ , which solves the semi-discrete version of the limiting system (4.4):

$$\frac{\rho^{n+1} - \rho^n}{\Delta t} + \nabla_x \cdot (\rho^n u^n) = 0, \quad \rho^n \mathcal{B}^n = 0. \quad (4.7)$$

To this end, we integrate the  $g_\varepsilon^n$  equation in (4.2) with respect to  $\xi$  to obtain

$$\frac{\rho_\varepsilon^{n+1} - \rho_\varepsilon^n}{\Delta t} + \nabla_x \cdot (\rho_\varepsilon^n u_\varepsilon^n) = 0.$$

Clearly, the limiting system as  $\varepsilon \rightarrow 0$  is the first equation in (4.7).

For the second equation in (4.7), we rewrite the  $u_\varepsilon^n$  equation in (4.2) as follows

$$\rho_\varepsilon^{n+1} \mathcal{B}_\varepsilon^{n+1} = \varepsilon \left[ \frac{\rho_\varepsilon^{n+1} u_\varepsilon^{n+1} - \rho_\varepsilon^n u_\varepsilon^n}{\Delta t} + \nabla_x \cdot (\rho_\varepsilon^n u_\varepsilon^n \otimes u_\varepsilon^n) + \nabla_x \cdot ((\omega_\varepsilon^n)^2 P_\varepsilon^n) \right],$$

where the right hand side is of order  $\mathcal{O}(\varepsilon)$ , thanks to the non-oscillatory condition (4.6). Taking the limit  $\varepsilon \rightarrow 0$ , we obtain  $\rho^{n+1} \mathcal{B}^{n+1} = 0$ .

It should be observed, that the AP property can be also verified for full discrete schemes. Detailed discretization can be found in, e.g. [21].

Note that the discrete non-oscillatory conditions (4.6) can be monitored during numerical simulations. Practically, instead of monitoring the oscillation on  $g_\varepsilon^n(x, \xi)$  for all  $x \in \Omega, \xi \in \mathbb{R}^d$ , we only need to keep track of the oscillation for  $\rho$  and  $P$ , namely the discrete version of conditions (3.4) and (3.6). The AP property is guaranteed to hold as long as there is no violation of the following assumptions

$$\max_x \frac{|\nabla_x \rho_\varepsilon^n|}{\rho_\varepsilon^n}, \max_x \frac{|\nabla_x P_\varepsilon^n|}{\rho_\varepsilon^n}, \max_x \nabla_x u_\varepsilon^n \leq C, \quad (4.8)$$

where  $C$  is a constant which does not depend on  $\varepsilon$ .

## 5. NUMERICAL EXPERIMENTS

In this section, we demonstrate the performance of the proposed schemes on a number of numerical examples. We note that the velocity scaling method in Section 2 and the resulting AP scheme in Section 4 are dimension independent. For simplicity, numerical simulations are performed on a 1-D by 1-D phase space, with periodic spatial domain  $\Omega = \mathbb{T} = [-\pi, \pi]$ . In particular, we consider the computation domain  $(x, \xi) \in [-\pi, \pi] \times [-6, 6]$ , and pick initial data such that  $R$  in (2.6) is much smaller than 6. So, the solution will vanish at the boundary. Unless otherwise specified, we always take  $N_x = 128$  and  $N_\xi = 64$  grid points in the phase space. We take  $\Delta t = \Delta x/20$  to satisfy the CFL condition, where  $\Delta x$  is spatial mesh size.

In this section, we focus on the 3-zone system (1.5). The aggregation system (1.3) can be solved similarly. The alignment kernel  $\phi$  of the 3-zone system is given by

$$\phi(x) = \frac{1}{\sqrt{1+x^2}}.$$

In the Examples 1–3 below, the interaction is modeled by the Morse potential

$$K(x) = -e^{-|x|/2} + e^{-|x|}.$$

**5.1. Example 1 – Validation of the assumptions.** The first test is to check whether the spatial non-oscillatory assumption (4.8) is valid for a typical initial value problem of (1.1). The rescaled system (4.1) is numerically solved subject to the initial data

$$g^0(x, \xi) = \rho^0(x)M(\xi), \quad \rho^0(x) = 1 + e^{-20(x-1)^2} + e^{-20(x+1)^2}, \quad u^0(x) = 0, \quad \omega^0(x) = 1,$$

where  $M(\xi) = \frac{1}{\sqrt{2\pi}}e^{-\xi^2/2}$ .

We track the time evolution of  $\max_x \frac{|\nabla_x \rho_\varepsilon|}{\rho_\varepsilon}$ ,  $\max_x \frac{|\nabla_x P_\varepsilon|}{\rho_\varepsilon}$  and  $\max_x |\nabla_x u_\varepsilon|$ , for different values of  $\varepsilon$ . The results shown in Figure 2 suggest that the assumption (4.8) is valid and the bounds are uniform with respect to  $\varepsilon$ .

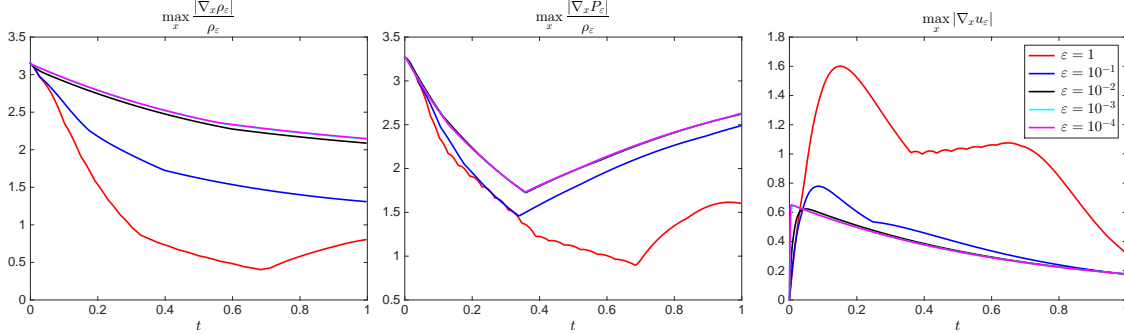


FIGURE 2. Example 1: The test on assumption 4.8. From left to right: the time evolution of  $\max_x |\nabla_x u_\varepsilon|$ ,  $\max_x \frac{|\nabla_x \rho_\varepsilon|}{\rho_\varepsilon}$  and  $\max_x \frac{|\nabla_x P_\varepsilon|}{\rho_\varepsilon}$  for different values of  $\varepsilon$ . The lines for  $\varepsilon = 10^{-3}$  and  $\varepsilon = 10^{-4}$  are almost overlapped.

**5.2. Example 2 – Consistency test.** In this example, we verify that the solution to the rescaled system (4.1) is consistent with the original system (1.1). The original system is integrated in time by the forward Euler method, while the rescaled system is evolved by the AP scheme (4.2). The original system is very difficult to solve for small  $\varepsilon$  and long time, due to the fact that the solution  $f_\varepsilon$  is approaching a singular delta function in velocity space. Hence, we take simulation  $\varepsilon = 1$  and run the simulations until the final time  $t = 0.7$  in this test.  $N_v = 512$  points are used in solving the original system (compare with  $N_\xi = 64$  for the rescaled system).

The following initial condition for the original system (1.1) is used,

$$f^0(x, v) = \frac{\rho^0(x)}{2\sqrt{0.4\pi}} \left( e^{-\frac{(v+\sin(x))^2}{0.4}} + e^{-\frac{(v-\sin(x))^2}{0.4}} \right), \quad \rho^0(x) = 1 + e^{-20(x-1)^2} + \frac{3}{2}e^{-20(x+1)^2},$$

which is equivalent to the rescaled system (4.1) solved subject to the initial condition

$$g^0(x, \xi) = \frac{\rho^0(x)}{2\sqrt{0.4\pi}} \left( e^{-\frac{(\xi+\sin(x))^2}{0.4}} + e^{-\frac{(\xi-\sin(x))^2}{0.4}} \right),$$

$$\rho^0(x) = 1 + e^{-20(x-1)^2} + \frac{3}{2}e^{-20(x+1)^2}, \quad u^0(x) = 0, \quad \omega^0(x) = 1.$$

Time snapshots of the density  $\rho_1(x)$  and the macroscopic velocity  $u_1(x)$  at different time  $t$  are compared in the top of Figure 3. The solutions to different systems are almost identical, demonstrating that the rescaled system is consistent with the original system. In the bottom of Figure 3, we show the distributions  $f_1(x, v)$  (left, solved from the original system) and  $g_1(x, \xi)$  (right, solved from the rescaled system) at time  $t = 0.7$ . As one can see,  $f_1(x, v)$  is getting concentrated in the velocity space, making it difficult to simulate with fixed grid points. In contrast,  $g_1(x, \xi)$  has a finite support in the rescaled velocity space  $\xi$  and a fixed grid in  $\xi$  can be used for the simulation.

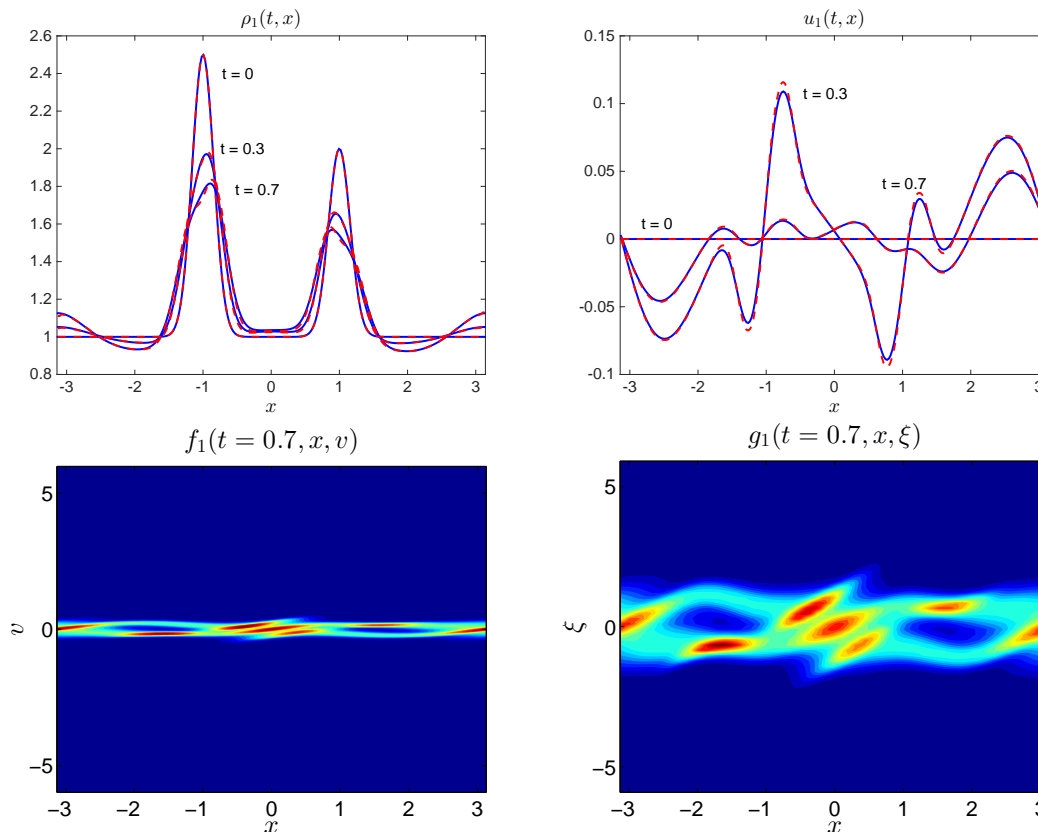


FIGURE 3. Example 2: Top left: the time evolution of  $\rho_1(x)$  solved from the original system (1.1) (blue solid lines) and the rescaled system (4.1) (red dashed lines). Top right: the time evolution of  $u_1(x)$  solved from the original system (1.1) (blue solid lines) and the rescaled system (4.1) (red dashed lines). Bottom left: the distribution  $f_1(x, v)$  at time  $t = 0.7$  solved from the original system (1.1). Bottom right: the distribution  $g_1(x, \xi)$  at time  $t = 0.7$  solved from the rescaled system (4.1).

**5.3. Example 3 - Asymptotic preserving test.** Now we test the AP property of the scheme (4.2). More specifically, we compare the solutions of (4.2) with vanishing

$\varepsilon$  to the solution of the limiting system (1.6). We use the following initial data

$$g^0(x, \xi) = \rho^0(x)M(\xi), \quad \rho^0(x) = 0.01 + e^{-20x^2}, \quad u^0(x) = 0, \quad \omega^0(x) = 1,$$

for the scheme (4.2). The limiting system (1.6) with initial condition  $(\rho^0, u^0)$  is well-posed with momentum conservation condition

$$\int_{\Omega} \rho(t, x)u(t, x)dx = 0, \quad \forall t \geq 0.$$

We refer to [9] for analysis and numerical schemes for the limiting system.

The comparison of the density  $\rho_\varepsilon(x)$  and macroscopic velocity  $u_\varepsilon(x)$  at time  $t = 1$  is given in Figure 4. Different  $\varepsilon$ 's are used for the scheme (4.2). The results clearly demonstrate that as  $\varepsilon$  vanishes, the solution obtained from (4.2) approach the solution to the limiting system, demonstrating the AP property of (4.2).

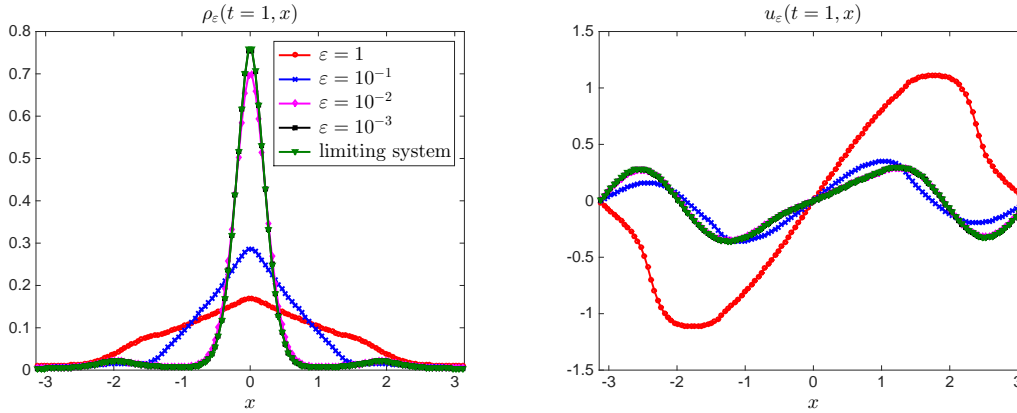


FIGURE 4. Example 3: The density  $\rho_\varepsilon(x)$  (left) and the macroscopic velocity  $u_\varepsilon(x)$  (right) at time  $t = 1$  computed by the scheme (4.2) with different  $\varepsilon$ 's are present, as well as that of the limiting system (1.6). The lines corresponding to  $\varepsilon = 10^{-3}$  almost overlap with the lines of limiting system.

**5.4. Example 4 – Application.** In this last example, we apply the numerical method developed in this work to an application problem. We solve the aggregation system (1.3) with a rescaled Morse potential

$$K(x) = -e^{-|x|} + e^{-2|x|}$$

and subject to the following initial data

$$\begin{cases} g^0(x, \xi) = \frac{\rho^0(x)}{2\sqrt{0.4\pi}} \left( e^{-\frac{(\xi+2)^2}{0.4}} + e^{-\frac{(\xi-2)^2}{0.4}} \right) \\ \rho^0(x) = 10^{-8} + e^{-40x^2}, \quad u^0(x) = 0, \quad \omega^0(x) = 1, \end{cases} \quad (5.1)$$

which describe two groups of agents in the same location moving to opposite directions.

The strength of interactions between agents are characterized by the value of  $\varepsilon$ . In Figure 5, we take  $\varepsilon = 1$ , hence a weak interaction is used. Time snapshots of the distribution  $g_1(x, \xi)$ , the density  $\rho_1(x)$ , the momentum  $\rho_1(x)u_1(x)$  and the scaling factor  $\omega_1(x)$  at different times are provided. It can be observed that the two groups continue moving toward opposite directions and eventually are separated from each other. The scaling factor  $\omega_1(x)$  decays to 0 uniformly in  $x$ . The alignment begins to dominate after a long time simulation, driving the momentum  $\rho_1 u_1$  to zero.

In Figure 6, we plot the solution of same problem with a strong interaction by taking  $\varepsilon = 10^{-4}$ . The effects of alignment and attraction/repulsion are much stronger than the free transport. The alignment plays a role in two aspects. First, it pushes  $\omega_\varepsilon$  to 0 immediately, describing all agents in the same location moving with the same velocity. This makes the two groups stick together. Second, after a long time, the alignment drives the momentum  $\rho_\varepsilon u_\varepsilon$  to zero for all  $x$ , hence forming a flocking pattern. The attraction/repulsion determines the shape of this pattern. In Figure 6, we also include the stationary solution (see e.g. [9]) of the limiting system (1.4) and note that it agrees very well with the long time profile of the aggregation system.

**Acknowledgment:** The work of A. Chertock was supported in part by NSF Grant DMS-1521051. A. Chertock and C. Tan acknowledge the support by NSF RNMS Grant DMS-1107444 (KI-Net).

## REFERENCES

- [1] Alexander V Bobylev, José A Carrillo, and Irene M Gamba. On some properties of kinetic and hydrodynamic equations for inelastic interactions. *Journal of Statistical Physics*, 98(3-4):743–773, 2000.
- [2] Marek Bodnar and Juna Jose Lopez Velazquez. Derivation of macroscopic equations for individual cell-based models: a formal approach. *Mathematical methods in the applied sciences*, 28(15):1757–1779, 2005.
- [3] José A Carrillo, Young-Pil Choi, Eitan Tadmor, and Changhui Tan. Critical thresholds in 1D euler equations with non-local forces. *Mathematical Models and Methods in Applied Sciences*, 26(01):185–206, 2016.
- [4] José A Carrillo, Massimo Fornasier, Jesús Rosado, and Giuseppe Toscani. Asymptotic flocking dynamics for the kinetic cucker-smale model. *SIAM Journal on Mathematical Analysis*, 42(1):218–236, 2010.
- [5] Nicolas Crouseilles, Hélène Hivert, and Mohammed Lemou. Numerical schemes for kinetic equations in the anomalous diffusion limit. part i: the case of heavy-tailed equilibrium. *SIAM Journal on Scientific Computing*, 38(2):A737–A764, 2016.
- [6] Nicolas Crouseilles, Hélène Hivert, and Mohammed Lemou. Numerical schemes for kinetic equations in the anomalous diffusion limit. part ii: Degenerate collision frequency. *SIAM Journal on Scientific Computing*, 38(4):A2464–A2491, 2016.
- [7] Felipe Cucker and Steve Smale. Emergent behavior in flocks. *Automatic Control, IEEE Transactions on*, 52(5):852–862, 2007.
- [8] Tam Do, Alexander Kiselev, Lenya Ryzhik, and Changhui Tan. Global regularity for the fractional Euler alignment system. *arXiv preprint arXiv:1701.05155*, 2017.
- [9] Razvan C Fetecau, Weiran Sun, and Changhui Tan. First-order aggregation models with alignment. *Physica D: Nonlinear Phenomena*, 325:146–163, 2016.
- [10] RC Fetecau and Weiran Sun. First-order aggregation models and zero inertia limits. *Journal of Differential Equations*, 259(11):6774–6802, 2015.

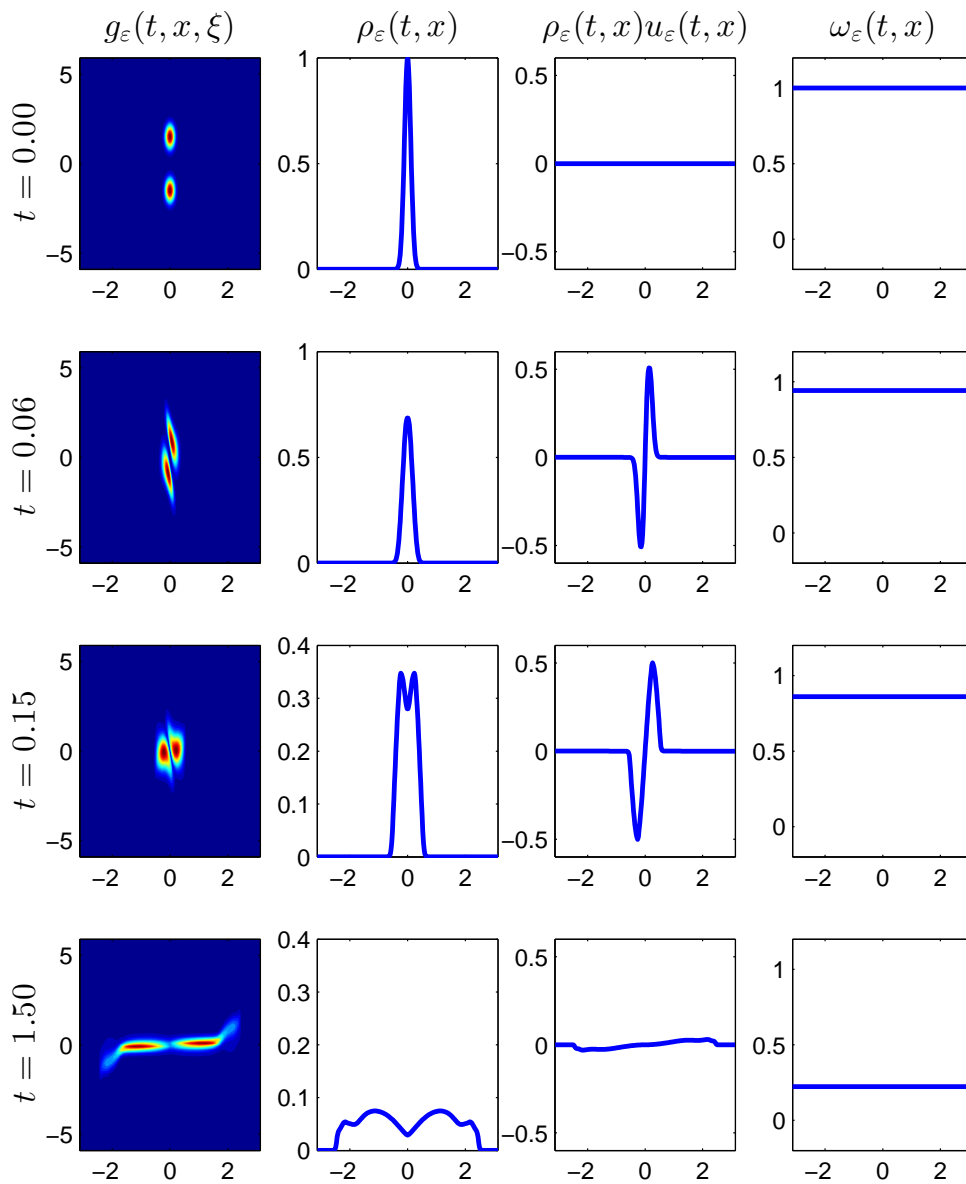


FIGURE 5. Example 4: Time snapshots of the solution to the aggregation system. From left to right: the distribution  $g_\varepsilon(x, \xi)$ , the density  $\rho_\varepsilon(x)$ , the momentum  $\rho_\varepsilon(x)u_\varepsilon(x)$  and the scaling factor  $\omega_\varepsilon(x)$ . In this test  $\varepsilon = 1$ .

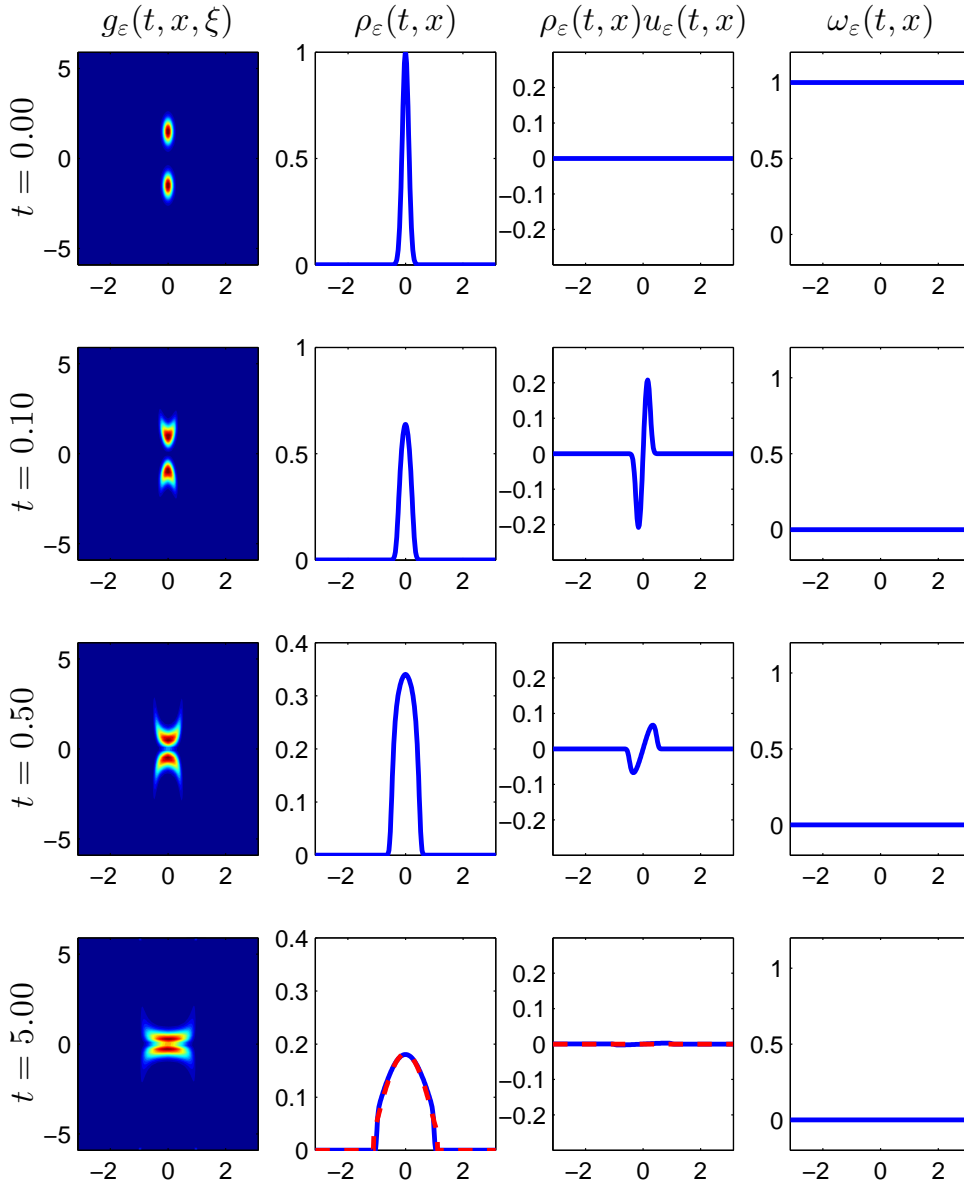


FIGURE 6. Example 4: Time snapshots of the solution to the aggregation system. From left to right: the distribution  $g_\varepsilon(x, \xi)$ , the density  $\rho_\varepsilon(x)$ , the momentum  $\rho_\varepsilon(x)u_\varepsilon(x)$  and the scaling factor  $\omega_\varepsilon(x)$ . In this test  $\varepsilon = 10^{-4}$ . The stationary solution  $\rho$  and  $\rho u$  of the limiting system (1.6) is illustrated by red dashed lines in the last row.

- [11] Francis Filbet and Thomas Rey. A rescaling velocity method for dissipative kinetic equations. applications to granular media. *Journal of Computational Physics*, 248:177–199, 2013.
- [12] Francis Filbet and Giovanni Russo. A rescaling velocity method for kinetic equations: the homogeneous case. *Proceedings Modelling and Numerics of Kinetic Dissipative Systems*, page 11, 2004.
- [13] Thierry Goudon, Shi Jin, Jian-Guo Liu, and Bokai Yan. Asymptotic-preserving schemes for kinetic-fluid modeling of disperse two-phase flows. *Journal of Computational Physics*, 246:145–164, 2013.
- [14] Thierry Goudon, Shi Jin, Jian-Guo Liu, and Bokai Yan. Asymptotic-preserving schemes for kinetic-fluid modeling of disperse two-phase flows with variable fluid density. *International Journal for Numerical Methods in Fluids*, 75(2):81–102, 2014.
- [15] Seung-Yeal Ha and Eitan Tadmor. From particle to kinetic and hydrodynamic descriptions of flocking. *Kinetic and Related Models*, 1(3):415–435, 2008.
- [16] Pierre-Emmanuel Jabin. Macroscopic limit of vlasov type equations with friction. *Annales de l’IHP Analyse non linéaire*, 17(5):651–672, 2000.
- [17] Shi Jin. Efficient asymptotic-preserving (ap) schemes for some multiscale kinetic equations. *SIAM Journal on Scientific Computing*, 21(2):441–454, 1999.
- [18] Shi Jin. Asymptotic preserving (AP) schemes for multiscale kinetic and hyperbolic equations: a review. *Lecture Notes for Summer School on "Methods and Models of Kinetic Theory" (M&MKT), Porto Ercole (Grosseto, Italy), June 2010. Rivista di Matematica della Università di Parma*, 3(17):177–216, 2012.
- [19] Alexander Mogilner and Leah Edelstein-Keshet. A non-local model for a swarm. *Journal of Mathematical Biology*, 38(6):534–570, 1999.
- [20] David Poyato and Juan Soler. Euler-type equations and commutators in singular and hyperbolic limits of kinetic Cucker–Smale models. *Mathematical Models and Methods in Applied Sciences*, 27(6):1089–1152, 2017.
- [21] Thomas Rey and Changhui Tan. An exact rescaling velocity method for some kinetic flocking models. *SIAM Journal on Numerical Analysis*, 54(2):641–664, 2016.
- [22] Craig W Reynolds. Flocks, herds and schools: A distributed behavioral model. *ACM SIG-GRAPH computer graphics*, 21(4):25–34, 1987.
- [23] Eitan Tadmor and Changhui Tan. Critical thresholds in flocking hydrodynamics with non-local alignment. *Phil. Trans. R. Soc. A*, 372(2028):20130401, 2014.
- [24] Changhui Tan. A discontinuous Galerkin method on kinetic flocking models. *Mathematical Models and Methods in Applied Sciences*, 27(7):1199–1221, 2017.
- [25] Chad M Topaz, Andrea L Bertozzi, and Mark A Lewis. A nonlocal continuum model for biological aggregation. *Bulletin of mathematical biology*, 68(7):1601–1623, 2006.
- [26] Li Wang and Bokai Yan. An asymptotic-preserving scheme for linear kinetic equation with fractional diffusion limit. *Journal of Computational Physics*, 312:157–174, 2016.
- [27] Li Wang and Bokai Yan. An asymptotic-preserving scheme for kinetic equations with anisotropic scattering: fat tail equilibrium and degenerate collision frequency. *preprint*, 2017.

ALINA CHERTOCK, DEPARTMENT OF MATHEMATICS, NORTH CAROLINA STATE UNIVERSITY, CAMPUS BOX 8205, RALEIGH NC 27695, USA

*E-mail address:* chertock@math.ncsu.edu

CHANGHUI TAN, DEPARTMENT OF MATHEMATICS, RICE UNIVERSITY, 6100 MAIN ST., HOUSTON TX 77005, USA

*E-mail address:* ctan@rice.edu

BOKAI YAN, DEPARTMENT OF MATHEMATICS, UNIVERSITY OF CALIFORNIA, LOS ANGELES, 520 PORTOLA PLAZA, LOS ANGELES, CA 90095, USA

*E-mail address:* yanbokai@gmail.com